www.czasopisma.pan.pl PAN POLSKA AKADEMIA NAUK www.journals.pan.pl

A R C H I V E S O F M E T A L L U R G Y A N D M A T E R I A L S

Volume 59 2014 Issue 4

DOI: 10.2478/amm-2014-0224

P. BOBROWSKI*, M. FARYNA*, A. BIGOS*, M. HOMA**, A. SYPIEŃ*, M. BIEDA*

THREE-DIMENSIONAL INVESTIGATIONS OF FINELY GRAINED MATERIALS

TRÓJWYMIAROWA ANALIZA MATERIAŁÓW DROBNOKRYSTALICZNYCH

Development of new materials requires application of sophisticated techniques to characterize microstructure in a very detailed way. The combination of Electron Backscatter Diffraction (EBSD) and Energy Dispersive Spectrometry (EDS) with Focused Ion Beam (FIB) are excellent examples of such techniques. They are based on serial sectioning of chosen region in the investigated sample followed by data acquisition using the dual-beam scanning electron microscope equipped with both electron and ion columns. Three kinds of samples have been investigated: a) are anticorrosive Ni-Mo coating on ferritic steel; b) the oxidized Crofer22 APU ferritic stainless steel; c) the Al 6013 aluminum alloy after complex plastic deformation. The obtained results allowed to analyze crystalline morphology, distribution of precipitates as well as to reconstruct internal structure of grains and grains boundaries geometry.

Keywords: 3D-EBSD; 3D-EDXS, Grain boundaries reconstruction

Rozwój nowoczesnych materiałów wymaga zastosowania coraz bardziej zaawansowanych metod takich jak techniki 3D-EBSD oraz 3D-EDXS, które polegają na wykonywaniu serii przekrojów przez badany obszar próbki i akwizycji danych z wykorzystaniem skaningowego mikroskopu elektronowego wyposażonego w źródło jonów. W prezentowanej pracy analizowano trzy rodzaje materiałów metalicznych: powłokę antykorozyjną na bazie niklu domieszkowanego molibdenem, wytworzoną metodą elektroosadzania na podłożu stalowym; powłokę tlenkową wytworzoną na powierzchni ferrytycznej stali nierdzewnej o komercyjnej nazwie Crofer 22APU; stop aluminium Al6013 poddany odkształceniu plastycznemu z wykorzystaniem metody Ko-Bo. Na podstawie danych pomiarowych uzyskanych z próbki antykorozyjnej powłoki Ni-Mo wykonano rekonstrukcję jej mikrostruktury oraz przeprowadzono analizę tekstury. W przypadku próbki stali Crofer 22APU przeprowadzono rekonstrukcję geometrii granic międzyziarnowych w materiale podłoża oraz wykonano analizę rozkładu wybranych pierwiastków w warstwie tlenkowej wytworzonej na powierzchni stali. Dane eksperymentalne uzyskane z próbki stopu Al6013 umożliwiły przedstawienie trójwymiarowej mikrostruktury materiału oraz analizę rozmieszczenia wydzieleń i obszarów odkształconych plastycznie.

1. Introduction

Development of new materials requires the application of sophisticated experimental techniques to characterize microstructure at constantly improving lateral and spatial resolution. Among various techniques which enable visualization of microstructure at ultimate magnifications one can list Scanning Electron Microscopy (SEM), Transmission Electron Microscopy (TEM) and Atomic Force Microscopy (AFM). Modern microscopes, employing several additional techniques are equipped with advanced detectors and spectrometers. For example, in the case of SEM, Field Emission Gun ESM (FEG-SEM) equipped with secondary (SE) and backscattered electron (BSE) detectors, energy dispersive X-ray spectrometer (EDXS) and electron backscatter diffraction (EBSD) facility enable to collect a vast range of information about the analyzed sample allowing for its complete characterization. The EDXS provides qualitative and quantitative information about the chemical composition in microareas, while the EBSD facility collects local crystallographic orientation data.

The conventional SEM provides two-dimensional (2D) data about the sample microstructure, however in several cases, such an information is not sufficient enough to characterize the material in a complete manner. Analysis of the grain boundary geometry [1], as well as investigation of the shape and distribution of various phases within the material, such as pores [2] and precipitates, requires three-dimensional (3D) information about the microstructure. The existing methods, which provide 3D experimental data can be divided into two kinds, namely, nondestructive and destructive [3]. The nondestructive methods include techniques based on transmission of electrons, neutrons or electromagnetic radiation through the investigated sample. The latter ones include experimental methods based on serial sectioning of the sample and subsequent reconstruction of the investigated volume by use of a dedicated software. The serial sectioning can be carried out by cutting, mechanical polishing [4] or focused ion beam milling

* INSTITUTE OF METALLURGY AND MATERIALS SCIENCE, 25 REYMONTA STR., 30-059 KRAKÓW, POLAND

** FOUNDRY RESEARCH INSTITUTE, 73 ZAKOPIAŃSKA STR., 30-418 KRAKÓW, POLAND

[5, 6]. In recent years, dual-beam microscopes employing FIB milling has become increasingly popular. The liquid metal ion source (the Ga^+ is most frequently used) produces an ion beam of highly energetic ions, which interacts with a sample and sputters surface atoms. By use of finely focused beam, it is possible to prepare cross sections through the sample with accuracy of few tens of nanometers. Application of the FIB technique to materials science was widely described by Orloff et al. [7]. The FIB-SEM device enables full automation of the slice milling and data acquisition processes. As the BSE, EBSD and EDXS signals are most frequently used for collecting of 3D data, the relevant experimental techniques are named FIB-SEM, 3D-EBSD and 3D-EDXS, respectively.

Experimental results presented in this paper describe the application of the 3D-EBSD and 3D-EDXS techniques for microstructure analysis of a) the anticorrosive Ni-Mo coating on ferritic steel; b) the oxidized Crofer22 APU ferritic stainless steel; c) the Al 6013 aluminum alloy after complex plastic deformation.

2. Experimental procedure

During the experiment, the sample was moved repeatedly between two positions. In the first one (FIB position), a slice of material was milled away, while in the second position, the experimental data (EBSD and EDX elemental maps) were collected. The geometrical setup of the microscope, which was used in this research research is shown in Fig. 1. When a pre-tilted holder was used, only the rotation of the sample about the tilted axis by 180° was needed. The 3D-EDXS and 3D-EBSD measurements were carried out at the sample's edge between two perpendicular surfaces. Such a setup facilitated the access to the region of interest (ROI) and required shorter ion milling reducing the experimental time significantly. Fig. 2 shows the SEM image of the ROI prepared for the experiment.

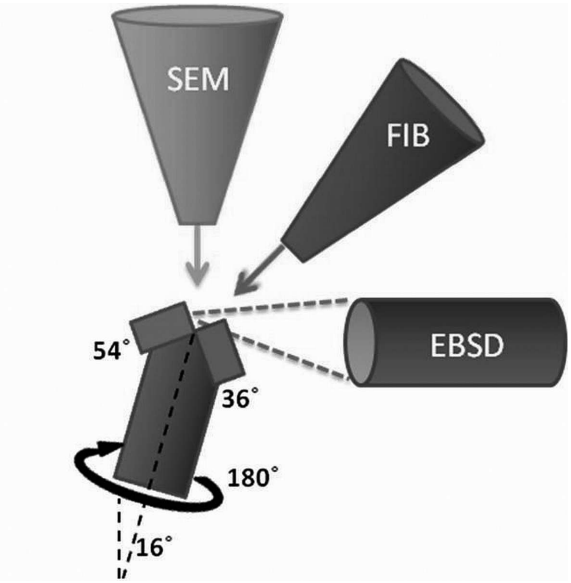

Fig. 1. Scheme of the geometrical setup of the FIB-EBSD tomography

The black rectangle marks the area from which the data was collected and two circular fiducial markers were used to adjust the samples position after each shift in the microscope chamber. The triangular trenches located on both sides of the ROI were milled to prevent shadowing of the investigated area.

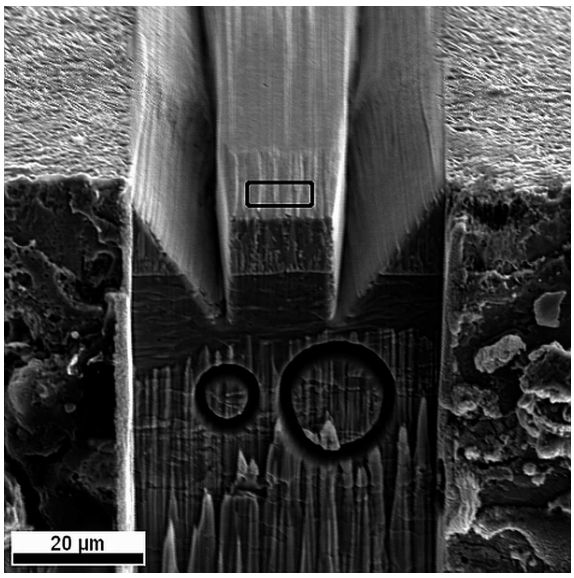

Fig. 2. Secondary electrons image of the ROI (marked by the black rectangle). Triangular trenches were milled to avoid shadowing. Circular fiducial markers were used in order to correct the position of the sample after each shift

In the case of the Ni-Mo alloy, the electron beam current and the accelerating voltage were set to 8 nA and 15 kV, respectively. These values were optimized to reduce the electron interaction volume and to improve the physical spatial resolution of EBSD. For the two other kinds of samples, namely Crofer 22 APU and Al 6013 alloy, the beam current and the accelerating voltage were set to 16 nA and 20 kV. These values resulted from the necessity to apply overvoltage sufficient to excite spectral lines of all the elements present in the investigated materials and to generate a large number of X-ray photons required for the EDXS analysis. Accelerating voltage of the ion beam was set to 30 kV for all of the investigated samples in order to obtain the optimum sputtering rate during slice milling. Jon beam current varied between 1 nA and 5 nA during the preparatory milling and slice milling, respectively.

3. Results and discussion

3.1. The 3D microstructure of the Ni-Mo alloy

Nickel-based coatings containing refractory metals such as molybdenum are a promising alternative to chromium layers, which are used in the automotive industry for improvement of corrosion protection and wear resistance. The main disadvantage of chromium coatings is the use of Cr^{6+} ions in the manufacturing process. These cations are highly toxic and should be removed from technological processes. Thus, there is a strong need to develop metallic films which could provide a satisfactory alternative to chromium coatings. The microstructure of Ni-based coatings depends strongly on the deposition method and requires extensive investigations to correlate the microstructure of the deposit with the parameters of manufacturing process.

The investigated material was electrochemically deposited from aqueous solution containing analytical grade purity chemicals: $Na_3C_6H_5O_7$, $NiSO_4$, Na_2MoO_4 [8]. A ferritic steel electrode was used as a substrate for electrodeposition. The process was carried out under galvanostatic conditions with the electric current density of 4 A/dm^2. The concentration of Mo addition in the sample was 5 at%. A square sample of 3×3 mm cut from the circular electrode was used for subsequent investigations.

Preliminary microstructure examination of the Ni-Mo coating, carried out on the cross-sections of the electrodeposited layer, revealed that the deposit is composed of elongated grains. A typical Inverse Pole Figure (IPF) map shows a distribution of local orientation of particular crystallites (Fig. 3). The stainless steel substrate can be seen in the upper part of the map. The Ni-Mo coating layer was composed of elongated grains growing perpendicularly to the substrate surface. However, in order to obtain the exact information about the size and shape of the grains within the investigated layer, the three-dimensional analysis of the microstructure was required.

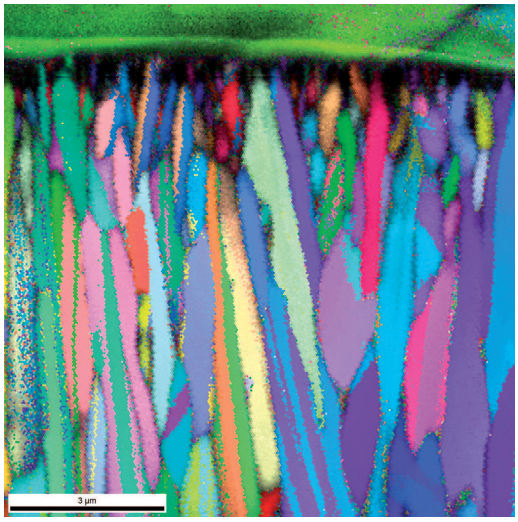

Fig. 3. Single inverse pole figure map acquired from the cross section of the Ni-Mo coating

The ROI dimensions during the 3D-EBSD measurement were 12×10×6 μm. The sample was scanned by electron beam with the step size of 100 nm on a square grid pattern. The distance between consecutive slices was also 100 nm to obtain cubic data voxels of 100×100×100 nm. Three-dimensional reconstructions of materials microstructure were carried out using the TSL OIM 5.0 Analysis software.

The 3D reconstruction revealed that the electrodeposited material consisted of columnar grains of ca. 1 μm in diameter on transverse section (Fig. 4). The detailed analysis of the samples' microstructure revealed that the grains were not ideally parallel to each other but they were tilted and twisted with respect to the substrate surface normal. Additionally, it was found that most of the grains had a similar crystallographic orientation, with the [111] direction almost parallel to the substrate surface normal. To confirm that this observation, taken from relatively small volume, is representative for the entire sample, a large 2D IPF map was collected from 20x20 μm cross section parallel to the coating surface (Fig. 5). Based on both 2D and 3D data, pole figures along the surface normal for [001] and [111] directions were calculated (Fig. 6). The comparison of two sets of pole figures showed that there was a relatively good agreement between 2D and 3D data. It is evident that crystallites of the deposited material grow parallel to the [111] crystallographic direction, contrary to [001] direction leading to a texture formation in the Ni-Mo deposits. Such a microstructure is uncommon for electrodeposited materials containing refractory metals. Literature [9,10] suggests that the addition of high melting metal causes grain refinement and leads to formation of nanocrystalline or amorphous structure. The mechanism of formation of large, columnar grains is unknown. Such a microstructure is not desired due to unfavorable mechanical properties. When the material is subjected to mechanical load, it may crack along the boundaries of columnar grains, leading to exposure of the steel substrate to external environment. Further experiments are required to establish the cause for formation of columnar grains in the electrodeposited material.

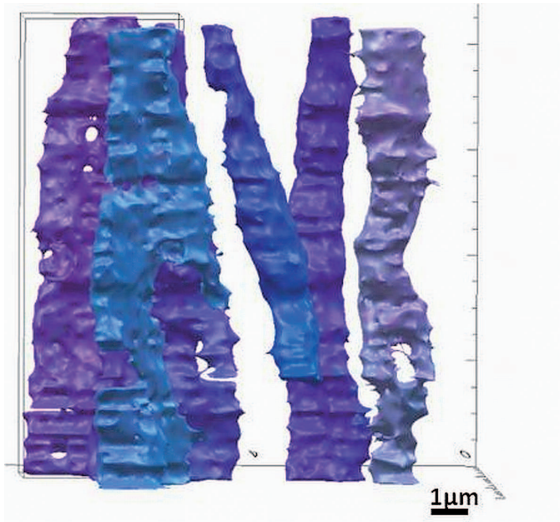

Fig. 4. 3D reconstruction of columnar Ni-Mo crystallites

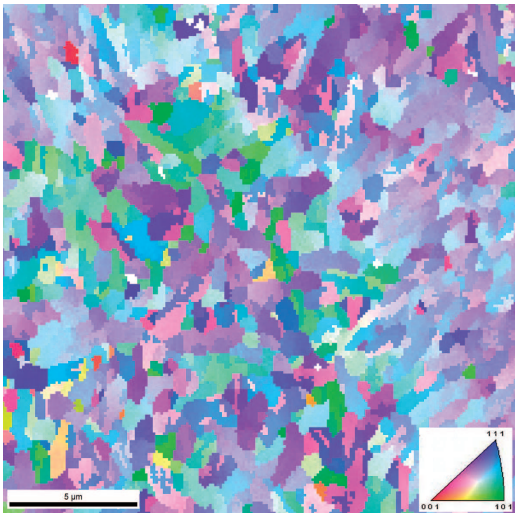

Fig. 5. 2D inverse pole figure map acquired from the cross section of the Ni-Mo coating parallel to the ferritic steel substrate

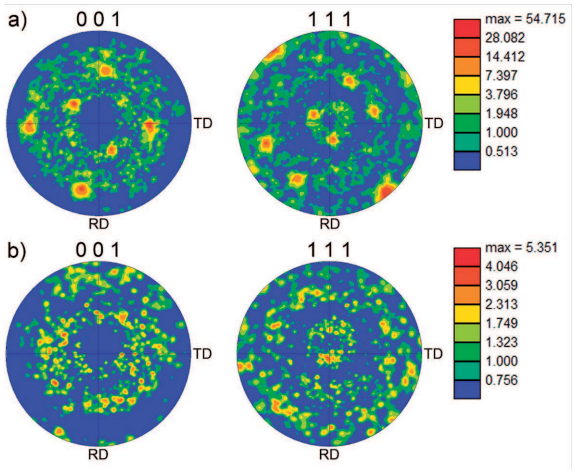

Fig. 6. Pole figures of the Ni-Mo coating calculated from a) 2D, b) 3D data

3.2. Investigation of the Crofer 22 APU stainless steel by 3D-EBSD and 3D-EDXS techniques

Crofer 22 APU is a high-temperature ferritic stainless steel developed especially for application in Solid Oxide Fuel cells (SOFC). It is thermodynamically stable [11,12] and possesses low electrical resistivity (1.15 $\mu\Omega$m [13]) compared to other materials. Its thermal expansion coefficient by fairly similar to the one of ceramics used for high-temperature fuel cells in the temperature range from ambient up to 900°C. The steel is characterized by excellent corrosion resistance at elevated temperatures [14], low rate of chromium evaporation ($1.5{\cdot}10^{-11}$kg/s·m^2), low coefficient of thermal expansion ($1.19{\cdot}10^{-5}$ K^{-1}) and good electrical conductivity of the chromium oxide layer forming on the materials' surface [13]. The FIB-SEM serial sectioning experiment was carried out to investigate the structure of chromium oxide layer formed on the steel substrate. Application of the FIB enabled the analysis of the oxide composition throughout the layer by sequential removal of the oxide until the clean steel substrate was revealed. Additionally, since the material consisted of large, undeformed grains, an experiment in the bulk of the steel was carried out to analyze the structure of grain boundaries within the material.

A sample of 10×10×0.5 mm was cut from a sheet of steel. Material was cleaned by electropolishing to obtain smooth surface adequate for EBSD measurements and subsequently oxidized for 12 h at 800°C. Such a procedure enabled to manufacture sample with relatively large grain size and equilibrium structure of grain boundaries, required for microstructure investigations by use of the 3D-EBSD technique. The reconstruction of grain boundary network was carried out using the Amira 5 Resolve RT software.

The 3D microstructure investigations were performed both inside the sample as well as on its surface. Figure 7 shows the 3D reconstruction of grain boundary network in the volume with dimensions of 10×8×8 μm, which was scanned with the step size of 100 nm and slice thickness of 100 nm. The reconstruction was accomplished by application of the marching cube algorithm [15]. The analysis of the 3D reconstruction showed that the investigated sample consisted of relatively large grains, none of which was entirely enclosed within the sampled volume. Grain boundaries formed large flat surfaces characteristic for an advanced level of the recrystallization process. Figure 8 shows the 3D visualization of elements distribution within the analyzed oxide layer with dimensions of 20×15×5 μm and voxel size of 100 nm. Distribution of oxygen (red areas) and chromium (green areas) are not homogenous, what indicates that several types of chromium oxide may be present within the layer. The blue areas in the Figure 8 show the location of steel substrate under the oxide layer. The EBSD data collected from the steel areas during the same experiment was used for the reconstruction of the sample surface morphology. Figure 9 shows the 3D visualization of the sample's surface, revealing that the steel surface, which was originally smooth due to electropolishing, became rough after oxidation process. Unfortunately, during the EBSD measurements most of the oxide crystallites did not produce any indexable patterns due to the fact that their size was below a physical spatial resolution of the EBSD technique. However, some information about the oxide layer was obtained due to the 3D-EDXS measurements.

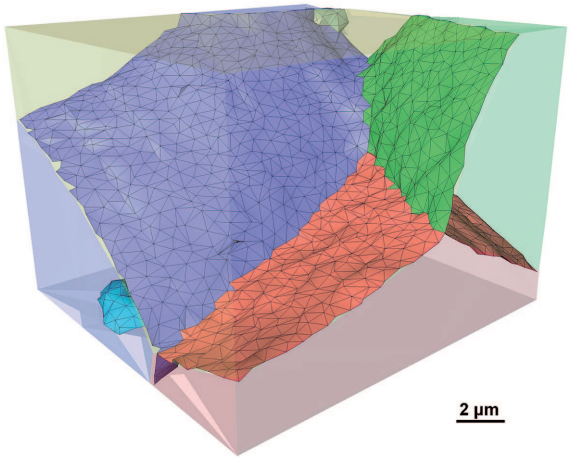

Fig. 7. 3D reconstruction of the grain boundary geometry in the Crofer 22 APU steel

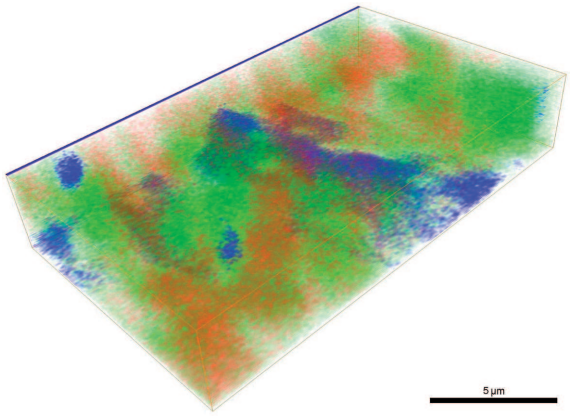

Fig. 8. 3D distribution of elements within oxide layer; blue color represents iron, green – chromium, red – oxygen

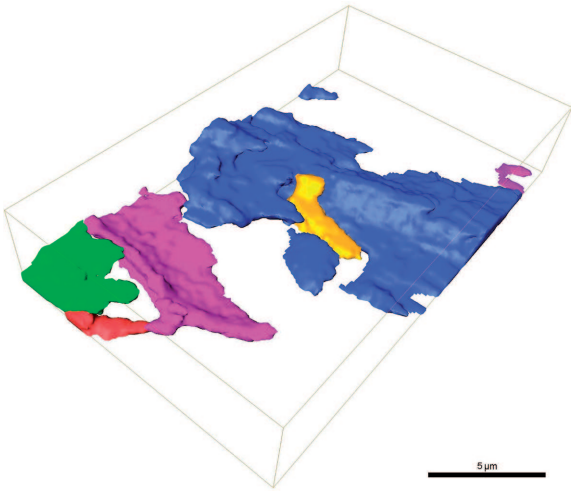

Fig. 9. 3D reconstruction of the sample surface. Visible crystallites were identified as ferritic steel substrate

3.3. Application of the 3D-EBSD and 3D-EDS techniques to the microstructure analysis of the Al 6013 alloy after severe plastic deformation by the KoBo extrusion process

The Al 6013 alloy with deformed microstructure was obtained by use of the KoBo [16] method, which combines a regular, uniaxial extrusion with rotation of the extrusion dye. Aluminum alloy 6013 after proper heat treatment possesses a relatively uniform bimodal distribution of stable fine ($<<1\mu$m) and coarse ($>1\mu$m) particles. These particles are of special interest in the studies of deformation and recrystallization processes, since they allow to obtain ultra-fine crystalline material with good combination of mechanical properties. Earlier investigations of aluminum alloy 6013 after cold rolling were presented in [17, 18]. Due to the complex nature of the strain in the KoBo method and different microstructures in transverse and longitudinal cross sections of deformed sample, the material is difficult for characterization based only on two-dimensional cross-sections through the sample. Therefore, 3D approach seems to be a useful solution for this experimental problem.

For the example presented here, a cylindrical sample, 1 mm thick and 4 mm in diameter, was cut from the rod and subsequently divided into two equal parts to facilitate the access to the central areas of the rod. The sample was preheated in the calorimeter in 235°C in order to achieve partial recrystallization with retained areas of high density of dislocations. Several 3D measurements were carried out along the radius of the rod. Figure 10 shows a stack of raw IPF maps obtained from a 10×10×5 μm volume located near the centre of the sample. The elongated shape of grains is easily visible. Based on the 3D reconstruction of a few selected crystallites a significant change of orientation was observed within particular grains (Fig. 11). Fig. 12 shows a misorientation profile calculated along a closed-loop line drawn in the IPF map (Fig. 13). Maximum misorientation between the points along the line and the origin is about 8 degrees, however only one recognizable grain boundary can be found along the point to-point plot. This fact can be explained by gradual changes of orientation within the material, caused by high density of dislocations introduced during plastic deformation. In the area shown in the Fig. 13, stacking of dislocations leads to formation of low angle boundaries. Additional information about deformed material can be obtained by use of the 3D approach, compared to the regular 2D measurements. Fig. 14 shows the 3D visualization of areas of high local misorientation within the investigated volume. Yellow and red colors indicate local misorientations higher than 3° and 5°, respectively. The presence of a recrystallized grain, surrounded by fields of high misorientation observed in the Fig. 14 (see arrow) suggests that in some regions of the material recrystallization process has begun. Observations confirmed inhomogeneous distribution of the regions of high density of dislocations. This is connected to the existence of small and large second-phase particles [18] which are responsible for materials behavior during annealing. Further detailed investigations should be carried out to reveal the mechanism of this process.

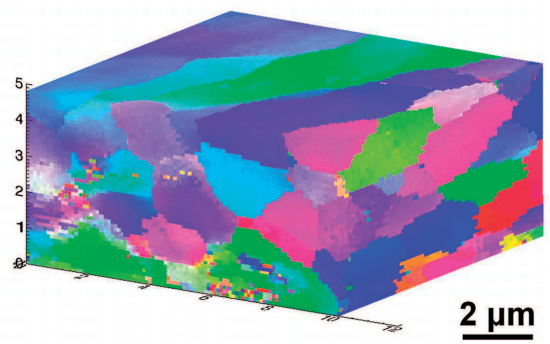

Fig. 10. Stack of IPF maps collected from the Al 6013 alloy

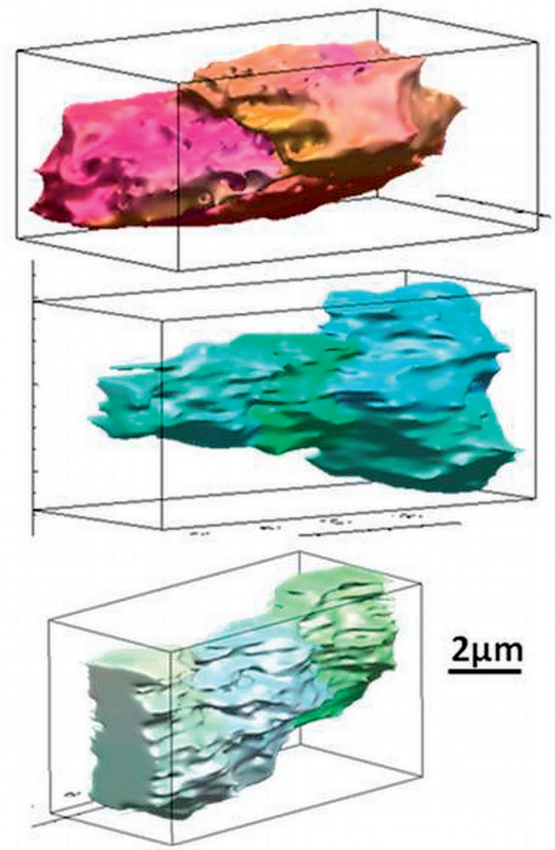

Fig. 11. 3D reconstructions of particular grains in the Al 6013 alloy

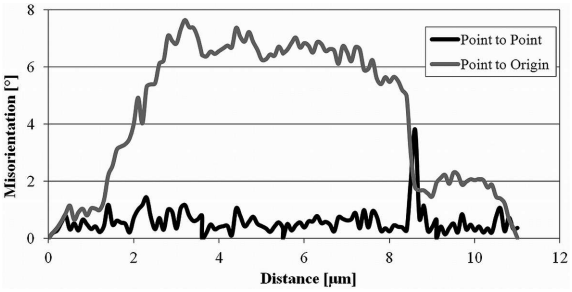

Fig. 12. Misorientation profile calculated along the line shown in Fig. 13

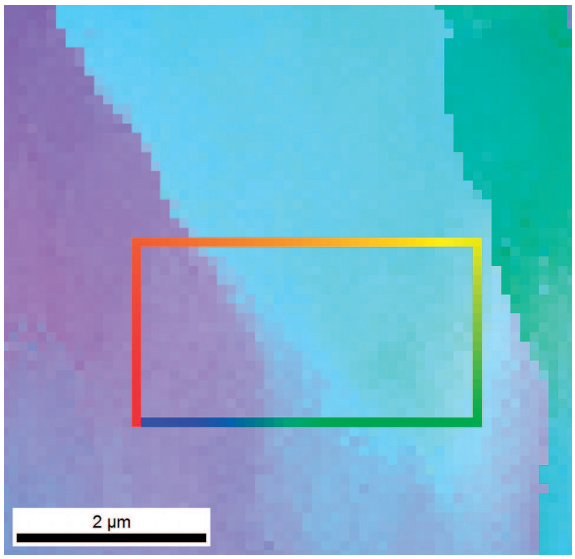

Fig. 13. IPF map with a closed-loop line drawn for misorientation profile calculation

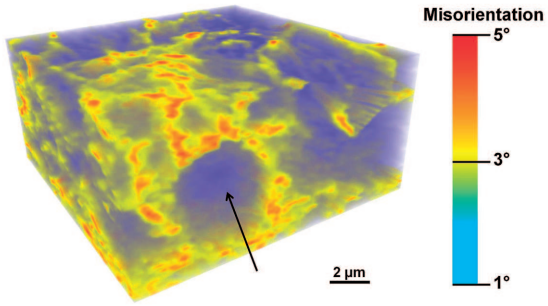

Fig. 14. 3D visualization of high misorientation areas

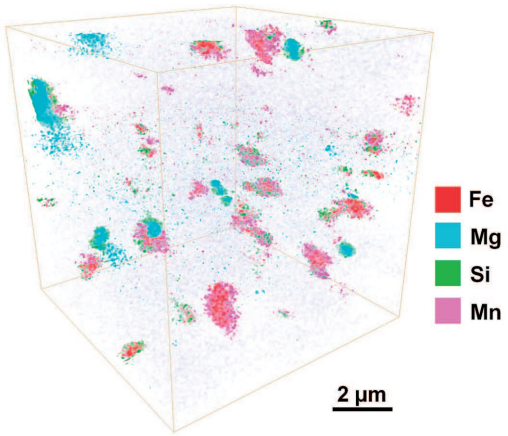

Fig. 15. 3D distribution of the precipitates containing large particles in the Al matrix

Fig. 15 shows the 3D reconstruction of precipitate distribution in the Al 6013 alloy obtained by use of the 3D-EDXS. Location of large precipitates in the Al matrix was shown. The 3D-EDXS technique is complementary to the 3D-EBSD, yielding information about the local chemical composition. It can be very helpful when the EBSD technique is not able to provide reliable experimental data, due to unknown crystallographic structure of intermetallic phases or close match of lattice parameters of phases existing in the sample. In such cases, phase identification can be successfully performed based on elemental distribution provided by the 3D-EDXS technique.

4. Summary

In the present paper, the capabilities of the 3D-EBSD and 3D-EDXS techniques were shown based on three selected examples. In the case of Ni-Mo coating electrodeposited on steel substrate, it was shown that the [001] direction is disfavored for the crystal growth. Crystallites grow favorably along the [111] direction forming columns of about 1 μm in diameter oriented perpendicularly to the substrate surface. Application of the FIB to investigations of the oxidized Crofer 22 APU steel enabled sequential removal of the oxide layer until the substrate was reveled. The analysis of chemical composition of the oxide layer revealed fluctuations in the amount of oxygen and chromium suggesting that the investigated layer is non-homogenous. Application of the 3D-EBSD technique to the Al 6013 alloy after plastic deformation enabled visualization of strain fields within the material. It was found that the investigated material contains undeformed grains surrounded by highly strained regions. The application of 3D-EDXS technique to the microanalysis of the Al 6013 alloy enabled identification of the precipitates in Al matrix.

Automated 3D orientation and elemental composition tomography performed in a dual-beam scanning electron microscope yields a vast amount of data for visualization of microstructure and microanalysis. This data provides much more information about the microstructure of investigated material than the traditional 2D experimental techniques.

Acknowledgements

The research is co-financed by the European Union under the European Social Fund, project no. POKL.04.01.01-00-004/10. Authors are grateful to PawełCzaja for careful reading of the manuscript.

REFERENCES

[1] A. Morawiec, On the frequency of occurrence of tilt and twist grain boundaries. Scripta Mater **61**, 438-440 (2009).

[2] H. Iwai, N. Shikazono, T. Matsui, Quantification of SOFC anode microstructure based on dual beam FIB-SEM technique. J Power Sources **195**, 955-961 (2010).

[3] J. Konrad, S. Zaefferer, D. Raabe, Investigation of orientation gradients around a hard Laves particle in a warm-rolled Fe_3Al-based alloy using a 3D EBSD-FIB technique. Acta Mater **54**, 1369-1380 (2006).

[4] M.V. Kral, G. Spanos, Three-dimensional analysis of proeutectoid cementite precipitates. Acta Mater **47**, 711-724 (1999).

[5] T.L. Matteson, S.W. Schwarz, E.C. Houge, Electron Backscattering Diffraction Investigation of Focused Ion Beam Surfaces. J Electron Mater **31**, 33-39 (2002).
[6] L. Gianuzzi, F. Stevie, Introduction to Focused Ion Beams, Springer 2005.
[7] J. Orloff, M. Utlaut, High Resolution Focused Ion Beams, Kluwer Academic 2003.
[8] A. Bigos, E. Beltowska-Lehman, P. Indyka, M.J. Szczerba, M. Kot, M. Grobelny, Electrodeposition and properties of nanocrystalline Ni-based alloys with refractory metal from citrate baths. Arch Metall Mater **58**, 247-253 (2013).
[9] M. Karolus, Rentgenowska metoda badania struktury materiałów amorficznych i nanokrystalicznych, Wydawnictwo Uniwersytetu Śląskiego 2011.
[10] E. Chassaing, N. Portail, A.F. Levy, G. Wang, Characterization of electrodeposited nanocrystalline Ni-Mo alloys. J Appl Electrochem **34**, 1085-1091 (2004).
[11] Z. Żurek, M. Homa, A. Jaroń, A. Stawiarski, Utlenianie stali Crofer22APU w atmosferze pary wodnej. Ochrona przed korozją, **54**, 349-351 (2011).
[12] ThyssenKrupp VDM GmbH, Crofer22APU Material Data Sheet No.4046, May 2010 Edition.
[13] A. Jaroń, Z. Żurek, M. Homa, A. Strawiarski, The structure of external surfaces of scale forming on Crofer 22APU steel in atmosphere containing H2/H2S, Arch Metall Mater **57**, 237-244 (2012).
[14] Z. Żurek, A. Jaroń, M. Homa, Morphology Analysis of the Scale Formed on Crofer 22APU Steel on Atmospheres Containing SO2, Oxid Met **76**, 273-285 (2011).
[15] Y. Yemez, F. Schmitt, 3D reconstruction of real objects with high resolution shape and texture, Image and Vision Computing **22**, 1137-1153 (2004).
[16] Korbel and Bochniak 1998, U.S. Patent 5.737.959, 2000 European Patent 0.711.210.
[17] M. Bieda, Investigations of fine grained metallic materials by means of orientation maps in transmission electron microscope, Sol St Phen **186**, 53-57 (2012).
[18] K. Sztwiertnia, J. Kawałko, M. Bieda, K. Berent, Microstructure of polycrystalline zine subjected to plastic deformation by complex loading, Arch Metall Mater **58**, 157-161 (2013).

Received: 20 January 2014.